J. Membrane Biol. 117, 285–298 (1990)

The Journal of
Membrane Biology

Electrophysiology of Cultured Human Lens Epithelial Cells

Kim Cooper, Peter Gates, James L. Rae, and Jerry Dewey
Departments of Physiology and Biophysics and Ophthalmology, Mayo Foundation, Rochester, Minnesota 55905

Summary. The lens epithelial K^+ conductance plays a key role in maintaining the lens ionic steady state. The specific channels responsible for this conductance are unknown. We used cultured lens epithelia and patch-clamp technology to address this problem. Human lens epithelial explants were cultured and after 1–4 passages were dissociated and used in this study. The cells from which we measured had a mean diameter of 31 ± 1 μm (SEM, n = 26). The resting voltage was −19 ± 4 mV (SEM, n = 10) and the input resistance was 2.5 ± 0.5 GΩ (SEM, n = 17) at −60 mV. Two currents were prominent in whole-cell recordings. An outwardly rectifying current was seen in nearly every cell. The magnitude of this current was a function of K^+ concentration and was blocked by 3 mM tetraethylammonium. The instantaneous current-voltage relationship was linear in symmetric K^+, implying that the outward rectificiation was due to gating. The current showed complex activation and inactivation kinetics. The second current seen was a transient inward current. This current had kinetics very similar to the traditional Na^+ current of excitable cells and was blocked by 0.1 μM tetrodotoxin. In single-channel recordings, a 150-pS K^+ channel and a 35-pS nonselective cation channel were seen but neither account for the macroscopic currents measured.

Key Words lens epithelium · whole-cell recording · cell culture · K^+ current · Na^+ current · ion channel

Introduction

The lens of the eye functions as an adjustable focusing element in the process of image formation on the retina. In order to maintain the transparency necessary to be an effective optical element, the lens has evolved several functional specializations. Two major cell types subserve these specialized functions: fiber cells and epithelial cells. Fiber cells form the bulk of the lens mass and produce a high concentration of protein that gives rise to the large refractive index necessary for focusing. The epithelial cells are the primary sites of control of the lens ion and water content. They are believed to have a high K^+ conductance and substantial Na/K pump activity. The two cell types are thought to coordinate their activities by gap junctional communication (Rae & Mathias, 1985).

Little is known about the specific properties of the K^+ conductance in lens epithelium in general and even less about the K^+ conductance of human lens. In epithelial tissues, the use of single-channel patch-clamp recording techniques has greatly advanced the understanding of ion transport mechanisms (Rae, 1984; Palmer & Frindt, 1986; Petersen, 1987, 1989; Welsh, 1987; Wills & Zweifach, 1987; Gogelein, 1988). However, the whole-cell patch-clamp configuration has only been used on a few epithelia (Petersen, 1987, 1989; DeCoursey, Jacobs & Silver, 1988; Hunter et al., 1988; Cooper, Rae & Gates, 1989; Fain & Farahbakhsh, 1989; McCann & Welsh, 1990). This technique allows the recording of macroscopic current from a single cell under conditions where the voltage and concentration of ions are under direct experimental control. We are applying the whole-cell recording technique to lens epithelia in an attempt to identify the channel responsible for controlling resting voltage in this tissue.

It is the goal of this paper to characterize the electrophysiological properties of human lens epithelia cultured in our laboratory with particular emphasis on K^+ conductance. This has been useful for three reasons. First, we have identified and characterized at least part of the resting K^+ conductance of this lens epithelium. Second, we have found several other conductances that may be of interest. Last, we have described results from our specific culture protocol. There now exist a number of different protocols for culturing human lens epithelium (Hamada & Okada, 1978; Reddan et al., 1982/83; Jacob, 1988; Reddy et al., 1988; Stewart et al., 1988; Nagineni & Bhat, 1989). It will be important to compare the transport properties of cells grown using these different protocols to determine the extent to which the cultured cells are a reasonable model for the primary tissue. This paper begins that process using whole-cell recording and single-channel patch-clamp methods.

Materials and Methods

Cell Culture

Human eyes, ranging in age from 32 to 94 years (mean 70.5), were obtained from the Mayo Foundation Eye Bank within 16 hr postmortem. The lens epithelium was isolated by standard dissection techniques. The resulting epithelial-monolayer preparations were attached to the bottom of 35-mm Falcon Primaria dishes and trimmed so that only the central region of the epithelium remained. This ensured that there was no contamination by ciliary epithelium. The explants were cultured in MEM medium (GIBCO) supplemented with 15% FBS (HyClone) and 1% penicillin/streptomysin (Sigma). The culture medium was replaced every three days. The cells were maintained at 37°C in a humidified atmosphere of 95% air-5% CO_2. The explants were passaged for the first time after approximately 15 days. Subsequent passages occurred about every 20 days with recordings being done only with cells from passages 1 through 4. All recordings have been made from passaged cells because we have not been able to produce healthy primary dissociates.

Dissociation

Cells were dissociated from confluent monolayers using 0.5% trypsin with 0.53 mM EDTA in HBSS (GIBCO) for approximately 10–15 min. The cells were then gently triturated from the dish, placed in a conical centrifuge tube, spun at 300 × *g* for 5 min, and resuspended in physiological saline. Cells from this suspension were used for one day's experiments.

Microscopy

Routine measurements of cell diameter were made using Hoffman modulation contrast microscopy and a calibrated eyepiece reticule. This measurement was made using a Nikon Diaphot inverted microscope outfitted with a Leitz 25× Fluorotar objective modified for Hoffman modulation.

Electrical Recordings

Whole-cell currents were recorded using standard techniques modified for ocular tissues (Rae & Levis, 1984; Rae, Levis & Eisenberg, 1988). Electrodes, constructed from Corning 7052 and 7760 glasses, were Sylgard (Dow Corning) coated and firepolished to a final resistance between 3 and 10 MΩ (mean 5.9 MΩ). With these electrodes, seals were obtained that ranged in resistance from 2.5 to 45 GΩ (mean 13.5 GΩ). Recordings were made, at room temperature, using modified Axopatch 1-B and 1-C patch clamps (Axon Instruments). All data reported uses the convention that outward current (i.e., current leaving the cell) is positive. The data were digitized using either a TL-1 or an Axolab-1 12-bit AD/DA interface (Axon Instruments) and an IBM-AT computer. Data were analyzed with the PCLAMP software package (Axon Instruments) and with custom macros developed in Microsoft EXCEL.

Some whole-cell recordings were made using a modification of the perforated patch technique (Lindau & Fernandez, 1986; Horn & Marty, 1988; Rae & Cooper, 1990). Our version of this technique involves using amphotericin B in the pipette solution. The tip of the electrode is dipped into an amphotericin free solution and then the pipette is backfilled with an amphotericin-containing solution. This is done to ensure that the tip is free of amphotericin for the first 5 min or so since amphotericin interferes with seal formation. After achieving a gigohm seal, the amphotericin finally diffuses to the tip and partitions into the patch membrane. Amphotericin forms channels of 0.5-pS conductance in 150-mM salt solution and has an open probability that is voltage independent (Ermishkin, Kasumov & Potzeluyev, 1976). The partitioning of tens of millions of these channels into the patch membrane yields a low resistance path to the cell interior. The advantage of this technique over traditional whole-cell recording is that the amphotericin patch is only permeable to small anions and cations; thus, the cell does not lose important small soluble control molecules. Low access resistances (on the order of 10 MΩ) were commonly obtained within 10 min.

An additional advantage of the amphotericin technique is that it yields a more stable access resistance once it has fully partitioned. This increased stability is important when capacity and series resistance compensation are used. With the traditional whole-cell recording technique the access resistance is usually three to five times the electrode resistance initially, but often drifts to larger values with time. This necessitates frequent readjusting of the capacity and series resistance compensation circuits.

Single-channel recordings were made using the same glasses as the whole-cell recordings. Measurements were made using an Axopatch 1-C or an AIO2121 patch clamp (Axon instruments). Data were taken into a digital tape recorder constructed from a digital audio processor and a video cassette recorder (Bezanilla, 1985). The current records were digitized via a 12-bit A/D converter into a DEC 11/73 computer system and analyzed using a custom software package (Rae, Dewey & Cooper, 1989).

Solutions

The cells were bathed in a standard mammalian saline whose composition was: (in mM) 149 NaCl, 4.7 KCl, 2.5 $CaCl_2$, 5 HEPES and 5 glucose. The pH was 7.35 and the solution had an osmolality of 300 mosm/kg. Whole-cell recordings were made with an internal solution of the following composition: (in mM) 10 KCl, 140 Kmethanesulfonate, 2 EGTA and 5 HEPES at pH 7.00. In the perforated patch recordings, the pipette filling solution was obtained from a stock solution of amphotericin B (Sigma) at a concentration of 30 mg/ml (in DMSO) diluted to 120 μg/ml with intracellular solution.

Results

Resting Cell Properties

In most experiments, currents were recorded using the standard whole-cell recording configuration (Marty & Neher, 1983). In brief, after obtaining a gigohm seal, a small pulse of suction was applied which ruptured the cell membrane in the patch electrode. With the resulting whole-cell configuration, any current flowing across the cell membrane could be recorded by the patch-clamp electronics. The voltage necessary to hold the membrane current at

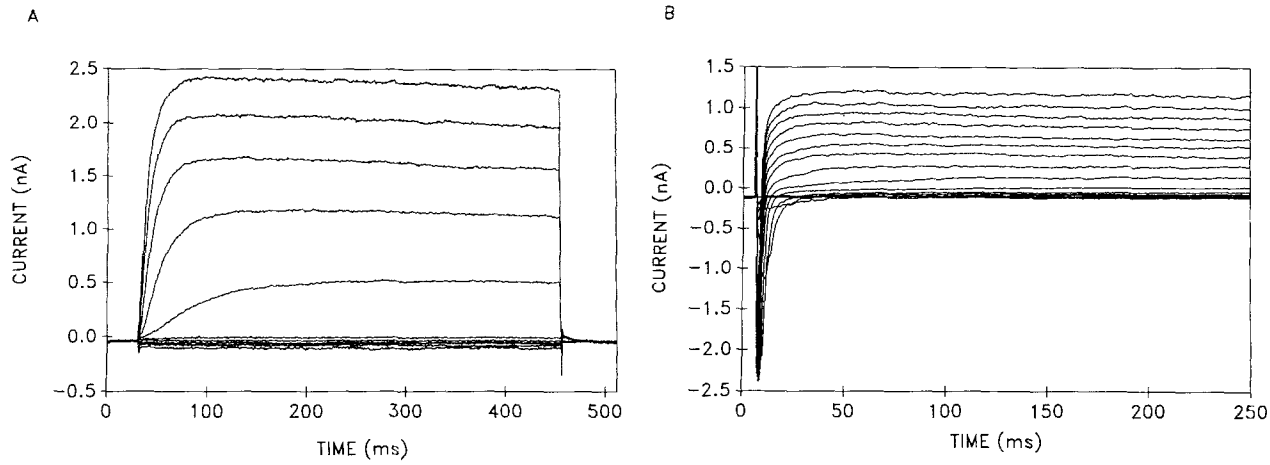

Fig. 1. (*A*) Currents in response to a multistep voltage protocol using traditional whole-cell recording. The bath contained normal physiological saline. This record is the average of three runs. Data were filtered at 1 kHz and sampled at 500 μsec/pt. (*B*) Currents in response to a multistep protocol similar to that in *A*, but using an amphotericin-perforated patch. The bath contained normal saline. This record is the average of 10 runs. Data were filtered at 1 kHz and sampled at 500 μsec/pt

zero was taken to be the cell resting voltage. Measurements were made within minutes of obtaining the whole-cell configuration. During this time the cell ionic contents should come to equilibrium with the pipette solution. A mean value for the resting voltage of -19 ± 4 mV (SEM, $n = 10$) was obtained. Cell input resistance was then determined by applying a 10-mV voltage step and measuring the resulting steady-state current. The input resistance was taken to be the ratio of these two numbers. For voltages near the holding voltage (usually -60 mV), the input resistance was 2.5 ± 0.5 GΩ (SEM, $n = 17$). Thus these cells have high resistance membranes in the negative voltage range under basal conditions.

Cell capacitance was measured using the Axopatch whole-cell compensation circuitry, yielding an average value of 50.0 ± 5.9 pF (SEM, $n = 23$). The mean diameter of the cells recorded from was 31 ± 1 μm (SEM, $n = 26$). If it is assumed that the cells are spherical, these two numbers yield an area specific capacitance of 1.7 μF/cm^2.

Currents

Using whole-cell and single-channel patch-clamp recording techniques, four types of currents were identified in these cells. Two types were K^+ currents: an outwardly rectifying macroscopic current and a channel which had a conductance of 150 pS at hyperpolarized voltages when 150 mM K^+ was in the pipette. A TTX-blockable macroscopic Na^+ current and a 35-pS nonselective cation (NSC) channel were also seen.

Whole-Cell Currents

Outwardly Rectifying K^+ Current. Figure 1*A* shows a series of whole-cell currents recorded in normal saline in response to a multistep voltage protocol. In this type of protocol the cell was maintained at a holding voltage (-60 to -80 mV) and then stepped through a series of voltages (12–16 steps) starting at -120 mV. The voltage steps were 250–500 msec in duration and were spaced at either 10- or 20-mV increments. Figure 1*A* was recorded with the traditional whole-cell technique while Fig. 1*B* was made using an amphotericin-perforated patch. In both cases, the steady-state current is much larger for depolarized voltages than for hyperpolarized voltages. This is referred to as outward rectification. In Fig. 1*B*, the transient inward current is a Na^+ current as shown below. Both currents were seen routinely with both types of whole-cell recording. The outwardly rectifying current was seen in nearly every cell and as shown below the current was carried predominantly by K^+. Since the outwardly rectifying current was the most commonly seen current in these cells and may be involved in determining resting voltage, a fairly detailed characterization of it is presented.

To demonstrate that the outward current was carried by K^+, whole-cell currents were recorded with several different K^+ concentrations in the bath. Figure 2 shows the currents in response to a 16-step protocol (20-mV spacing) from a holding potential of -60 mV. The bath contained a normal saline solution with 150 mM K^+ replacing the Na^+. With K^+ in the bath, nontransient inward currents during the pulses and transient inward currents fol-

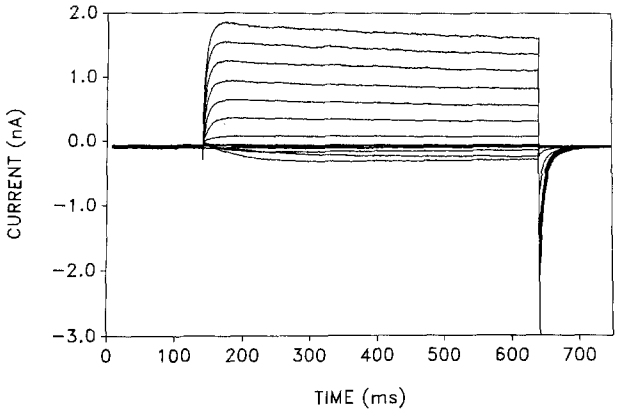

Fig. 2. Currents in response to a step protocol similar to that used in Fig. 1*A*, using a traditional whole-cell configuration. The bath contained a 150-mM K^+ physiological saline solution. This recording is the average of three runs, filtered at 1 kHz and sampled at 500 μsec/pt

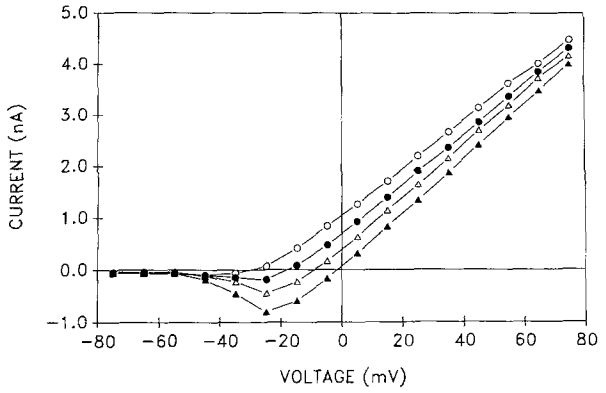

Fig. 3. Each curve represents the current at the end of a pulse from a step protocol similar to that used in Fig. 2. The curves were obtained in different bath K^+ concentrations as follows: open circles, 40 mM K^+; filled circles, 75 mM K^+; open triangles, 110 mM K^+; filled triangles, 150 mM K^+

Table 1.

K_o	V_{rev}	V_K	$V_{rev} - V_K$
150	0.0	0.0	0.0
110	−8.1	−8.0	−0.1
75	−18.0	−18.0	0.0
40	−33.7	−34.0	0.3

Measured reversal potential (V_{rev}) of the outwardly rectifying K^+ current compared to the Nernst potential for K^+. V_{rev} comes from data in Fig. 3. V_K is the computed Nernst potential.

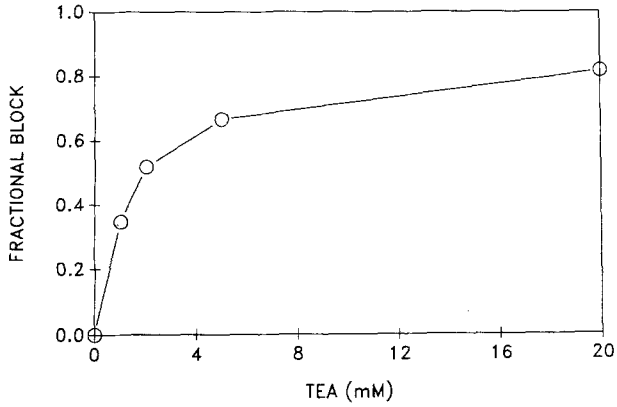

Fig. 4. Fractional block of outwardly rectifying K^+ current by TEA. Fractional block is defined by Eq. (1) in the text

lowing the pulses (tail currents) became measurable. Presumably, these currents were carried by the elevated bath K^+. In addition, it was evident from these curves that the outward current had not reached a steady state by the end of the pulses (500 msec). As shown later, this droop represents a slow inactivation process. Figure 3 shows the currents present at the termination of the voltage pulses from a protocol similar to the one used in Fig. 2. The outward rectification is clearly seen in these curves. Each curve was obtained with a different external K^+ concentration (40–150 mM). The magnitude of the inward current increased with increasing bath K^+ concentration as expected for a K^+ current. The K^+ selectivity was quantitated by comparing the reversal potential of the current with the calculated Nernst potential for K^+ (Table 1). The maximum deviation between these two numbers was only 0.3 mV. This corresponds to a P_K/P_{Na} ratio of 234.

Further evidence that this current was carried by K^+ came from investigation of the effect of channel blockers. Several traditional K^+ channel blockers were tested and tetraethylammonium (TEA) was found to be the most effective. Block was defined as follows:

$$B = 1 - \frac{I(\text{TEA})}{I}. \quad (1)$$

B is the fractional block at a given TEA concentration, I(TEA) and I are the maximum currents recorded in response to an 80-mV step with and without TEA, respectively. Figure 4 shows B for a range of external TEA concentrations. Half-maximal block occurred at a TEA concentration of 3 mM. The fact that B had not reached unity by 20 mM may be indicative of the presence of another conductance in this cell. The K^+ current was not substantially reduced by externally applied Cs^+ or Ba^{2+} in

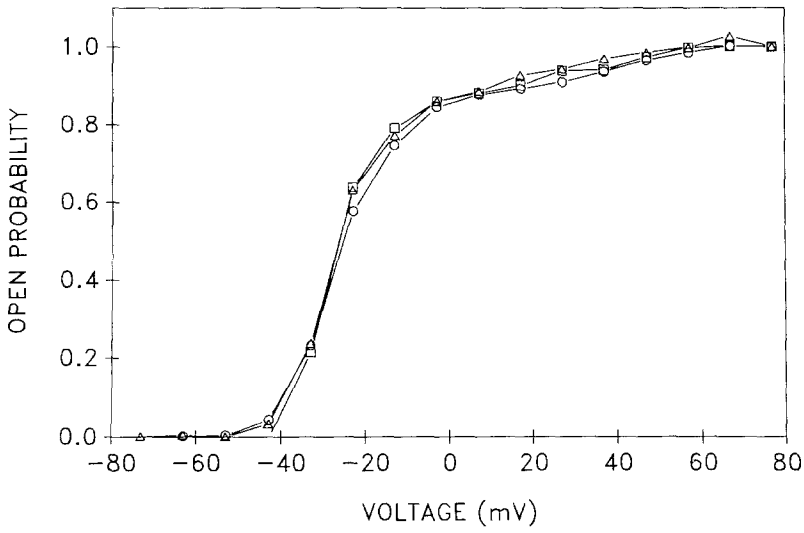

Fig. 5. Open probability (in absence of inactivation) of outwardly rectifying K^+ currents at various voltages. The open probability was determined from the ratio of tail currents as described in the text. The three curves were obtained with different holding voltages: squares, −40 mV; triangles, −60 mV; circles, −80 mV

the 1–20 mM range. The above data indicate that this current was carried predominantly by K^+.

It is of interest to know whether the rectification in this current was due to permeation or gating. This issue can be decided using data like that in Fig. 2. At any instant in time the macroscopic current (I) is given by:

$$I = N \cdot i \cdot p \tag{2}$$

where N is the number of channels in the cell, i is the current flowing through a single channel, and p is the probability that a given channel is open. This assumes that only one channel type is active. Rectification can be due to nonlinear voltage dependence in p and/or i (assuming that N does not change with voltage). To decide between these two possibilities, p was measured from an analysis of the tail currents. This measurement was made with voltage steps that were short relative to the time scale of inactivation. In Fig. 2 it is clear that more current flowed during the depolarizing voltage steps than at the holding voltage. However, on return to the holding voltage a transient inward current (tail current) flowed. With the symmetrical K^+ solution used in the experiment, there was a substantial driving force for K^+ at the holding voltage. This was reflected in the large initial value of the tail current associated with return from the more depolarized voltage steps. The subsequent decay of the tail current represented the return of the open probability from a high value at the depolarized voltage to the low value associated with the holding voltage. Examination of the tail currents showed that for voltage steps more depolarized than 80 mV, the peak of the tail current saturated. This implies that the open probability during the preceding step had reached unity. By taking the ratio of the peak of the tail current at one voltage to the maximum peak tail current, p at that voltage is obtained.

A series of open probabilities calculated in this way is shown in Fig. 5. The three curves represent data taken with three different holding voltages as a test of the consistency of the analysis. These are not true steady-state open probabilities because the inactivation process had not reached its steady state. They represent the probability of being in the open state given that the channel had not had time to reach the inactivated state. These open probabilities can be used to determine the instantaneous current-voltage relationship. By dividing the current at the end of a pulse by the corresponding open probability determined at that voltage, the instantaneous current is obtained. This is shown in Fig. 6 (open circles). The result is equivalent to $N \cdot i$ of Eq. (2) and thus has the same shape as the single-channel current-voltage curve. Since the single-channel current-voltage relationship is linear in symmetrical K^+, the rectification in the whole-cell current must be due to gating, i.e., p in Eq. (2).

The instantaneous current-voltage relationship can be determined in another way. By stepping the voltage from the holding potential (−60 mV) to a large positive value (+80 mV) for a long enough time (40 msec), all the channels can be opened. A measurement of the peak of the tail current on return to some test voltage is then a direct measure of $N \cdot i$ at that test voltage. No correction is needed for p because the prepulse to +80 mV has driven p to unity. The instantaneous current-voltage relationship can be determined by performing this procedure over a wide range of test voltages (*see* Fig. 8*A*). Figure 6 (open triangles) shows a current-voltage relationship determined in this way. The curves

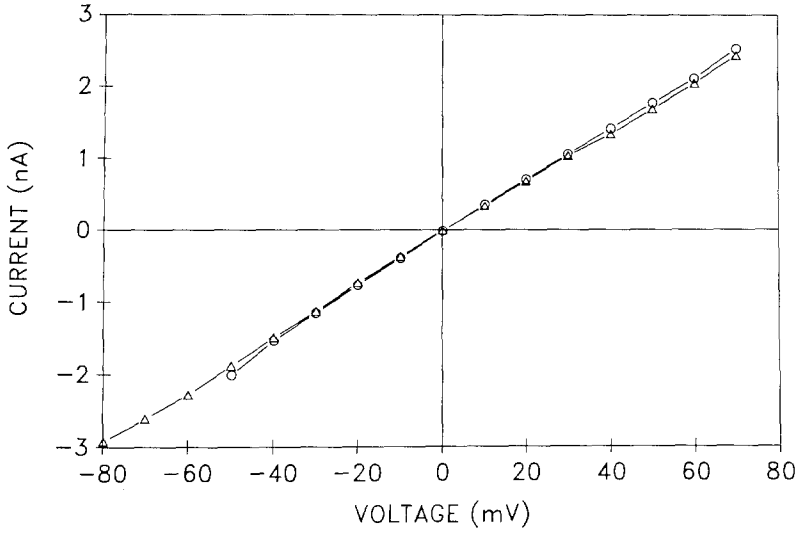

Fig. 6. Instantaneous current-voltage relationship of outwardly rectifying K^+ current. Circles: determined by dividing the 150-mM K^+ curve of Fig. 3 by the open probability in Fig. 5. Triangles: direct measurements of instantaneous currents using the protocol described in the text

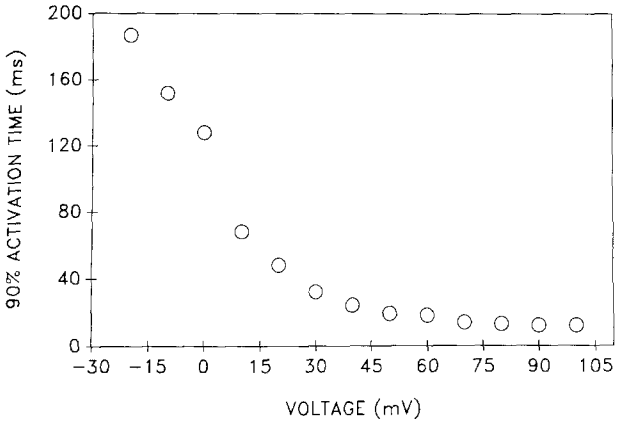

Fig. 7. Time to reach 90% of full activation measured from curves like those of Figs. 1 and 2

determined by the two techniques described above overlie one another.

Given the importance of gating in determining the rectification of this current, a rough characterization of its gating kinetics is useful. From Fig. 2, it is evident that the outwardly rectifying current had at least three voltage-dependent processes. When the voltage was stepped from the holding voltage to a voltage more positive than +20 mV, a time-dependent rise in current occurred (activation). This is due to a voltage-dependent increase in the number of open channels. The reverse of this process (deactivation) occurred on termination of the pulse and return to the holding potential. This process was seen as the time-dependent decay of the tail currents and was thus most easily measured in symmetric K^+ solutions. The third process was a slow decrease in current during a depolarizing pulse. This process, know as inactivation, was somewhat variable and clearly occurred on a time scale much longer than that of the pulses used in Fig. 2. Inactivation could only be removed by returning to a hyperpolarized voltage for a few seconds. This removal of inactivation represents a fourth process but was not visible in Fig. 2.

The voltage dependence of activation was determined by measuring the time to reach 90% of the peak current. This measure was chosen because the activation process was not well fit by a single exponential. As shown in Fig. 7, the time to reach 90% activation was strongly voltage dependent, decreasing by an order of magnitude as the transmembrane potential was depolarized over a 100-mV range. Figure 8*A* shows a series of whole-cell currents that demonstrate the voltage dependence of the deactivation process. The tail currents were fit with a single exponential to quantitate the major component of their voltage dependence. As with the activation process, a two-exponential fit was better but in this case the second component was small. Figure 8*B* shows the time constants derived from the fits as a function of voltage. Again, there was significant voltage dependence, with deactivation becoming slower at more depolarized voltages.

In Fig. 2 there is some evidence of inactivation but it obviously occurred on a time scale longer than the pulses used. To investigate inactivation more fully, cells were held at −80 mV, a voltage that gives fully activatable currents. From −80 mV, the voltage was stepped to more positive potentials for several minutes to allow the currents to inactivate. The result of one such experiment is shown in Fig. 9*A*. As with activation and deactivation, there were at least two time constants when the current was fit by a sum of exponentials. The time to reach 90%

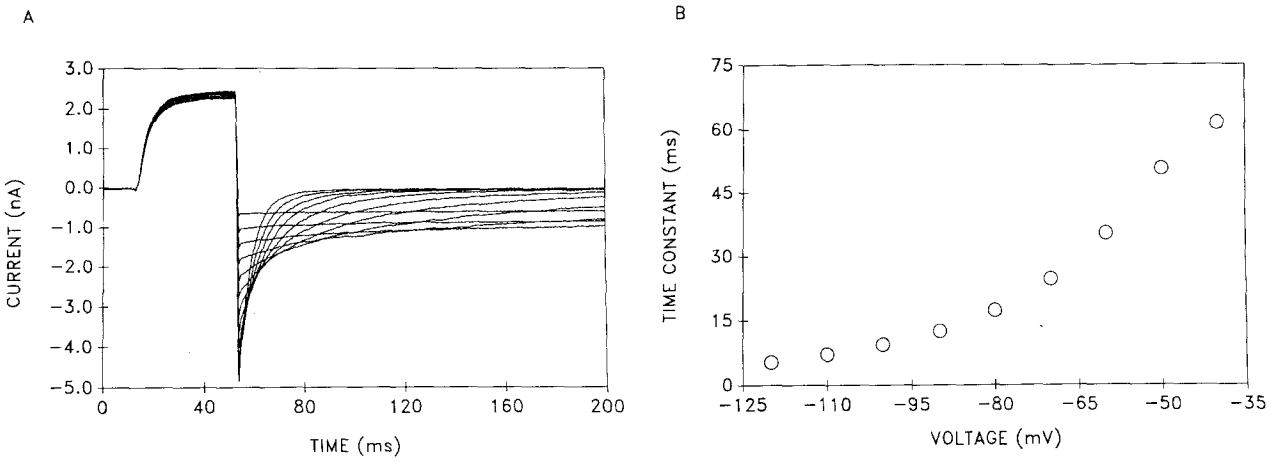

Fig. 8. (*A*) Currents recorded with traditional whole-cell technique. This protocol was designed to measure both the instantaneous current-voltage relationship and the time course of deactivation. The physiological saline in the bath contained 150 mM K^+. This figure is the average of two runs filtered at 1 kHz and sampled at 200 μsec/pt. (*B*) Time constants of tail currents from *A*

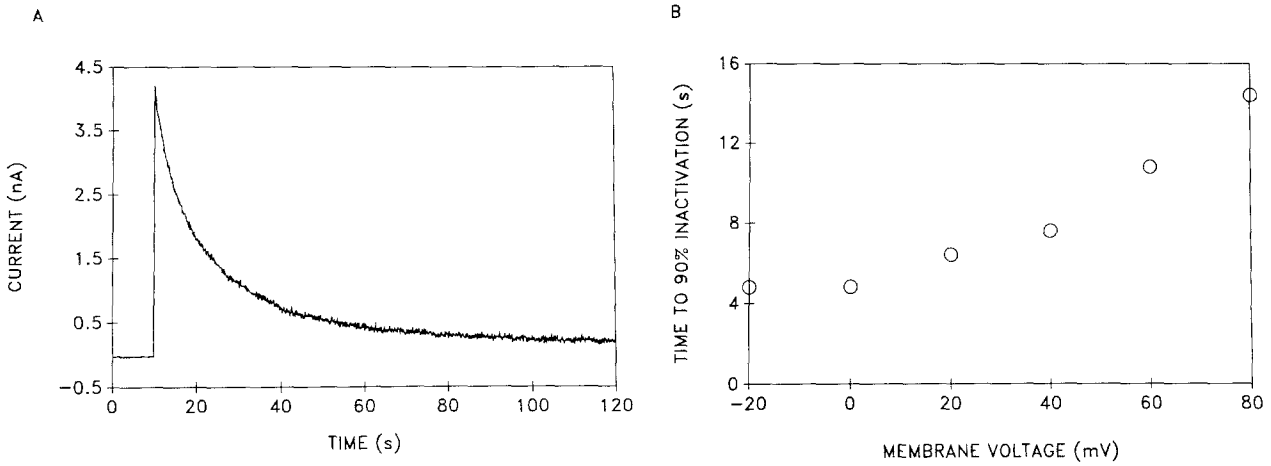

Fig. 9. (*A*) Current recorded with traditional whole-cell technique. This protocol was designed to measure the time course of inactivation. The bath contained normal physiological saline. No averaging was done in this experiment. The data were filtered at 20 Hz and sampled at 100 msec/pt. (*B*) Time to reach 90% of inactivation as a function of voltage

inactivation was a function of the step voltage as shown in Fig. 9*B*. Inactivation became slower at more depolarized voltages but was not as voltage dependent as the activation process.

A more complex protocol was used to measure the time course of the removal of inactivation. The cells were held for several minutes at 0 mV to give complete inactivation. The voltage was then stepped to a test value of −80 mV for various lengths of time to remove the inactivation. To assess the extent of recovery during this period, a short pulse to +80 mV was made. Following the short pulse to +80 mV, The voltage was returned to 0 mV and then the entire process was repeated at a different test voltage. Figure 10*A* shows the currents in response to a family of such pulses. The envelope of the peak of the currents shows the time course of recovery from inactivation. A series of recovery experiments is plotted in Fig. 10*B* for various test voltages. The time to 90% recovery from inactivation was weakly voltage dependent.

The kinetic behavior of this current can be approximately described by a three-state kinetic model which assumes that the channel can be in only one of three states: open, closed or inactivated.

$$C \underset{\beta}{\overset{\alpha}{\rightleftarrows}} O \underset{\delta}{\overset{\gamma}{\rightleftarrows}} I. \tag{3}$$

The rate constants (α, β, γ, δ) connecting the three states were derived from Figs. 7–10. Figure 7 was

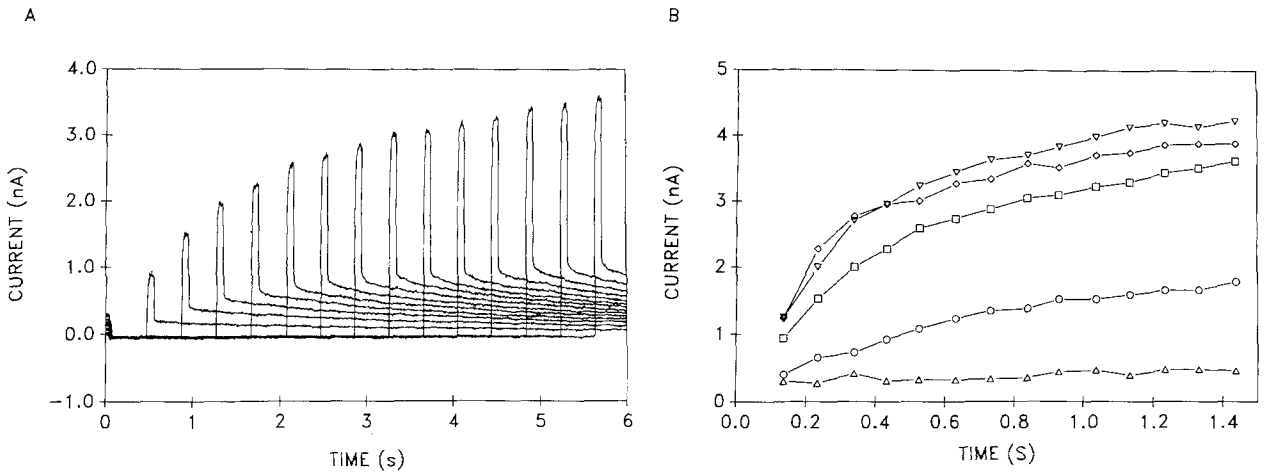

Fig. 10. (*A*) Protocol designed to measure the time course of removal of inactivation. The bath contained normal physiological saline. Currents were recorded with traditional whole-cell technique. No averaging was done in this experiment. The currents were filtered at 100 Hz and sampled at 4 msec/pt. (*B*) Envelope of peak currents from protocols like that in *A*. Traces represent different test voltages as follows: inverted triangles, −120 mV; diamonds, −100 mV; squares, −80 mV; circles, −60 mV; triangles, −40 mV

Table 2.

	A (sec^{-1})	B (mV)	C
α	11.00	−27	0.11
β	2.70	25	0.00
γ	1.00	33	2.00
δ	0.02	26	0.00

Constants that specify the voltage dependence of the rate constants as defined in Eq. (4).

assumed to be the inverse of α, Fig. 8*B* the inverse of β, Fig. 9*B* the inverse of γ, and δ was derived from the inverse of the rates calculated from Fig. 10*B*. In each case the rate constant was described by an equation of the form

$$\text{rate constant} = A/\{\exp(V/B) + C\} \quad (4)$$

where A, B, and C are constants unique to each rate. The constants are given in Table 2. The predictions of this model were determined for the various voltage protocols used by solving the set of differential equations derived from Eq. (3) using a Runge-Kutta algorithm (Press et al., 1986). Examples of the behavior of this model are shown in Fig. 11. In Fig. 11*A–C*, the results of the experiments shown in Figs. 2, 8*A*, and 10*A*, respectively, are simulated. From the voltage dependence of α and β, the results of Fig. 5 were calculated as shown in Fig. 11*D*. Clearly, this model produced currents that were quite similar to those observed experimentally.

Na^+ Currents. It was surprising to find fast inactivating inward Na^+ currents in about 25% of these cells. Evidence of such a current is apparent in Fig. 2*B*. Figure 12*A* shows an example of these currents with higher time resolution. The peak amplitude increased with more hyperpolarized holding potentials. The current could be reversibly removed by changing the bath to a Na^+-free solution. Figure 12*B* and *C* show that the currents were completely but reversibly blocked by 0.1 μM TTX. Such currents were seen in both traditional whole-cell recordings and in amphotericin-perforated patch recordings. The magnitude of the current was variable from cell to cell but did not correlate with time in culture or number of passages of the cultured cells.

Single-Channel Currents

Potassium Channel. Previous experiments from this laboratory on fresh monolayers of human lens epithelium have shown the existence of a Ca^{2+}-activated K^+ channel (*unpublished observations*). A similar channel appeared in recordings from these cultured dissociated human lens epithelial cells. Figure 13*A* shows a series of single-channel recordings at different voltages from an inside-out patch. The bath contained normal physiological saline and the pipette was filled with physiological saline in which the Na^+ had been replaced by K^+. The flickery kinetics and voltage dependence of channel opening are reminiscent of the Ca^{2+}-activated K^+ channel seen in the monolayers. Figure 13*B* is the current-voltage relationship obtained from these re-

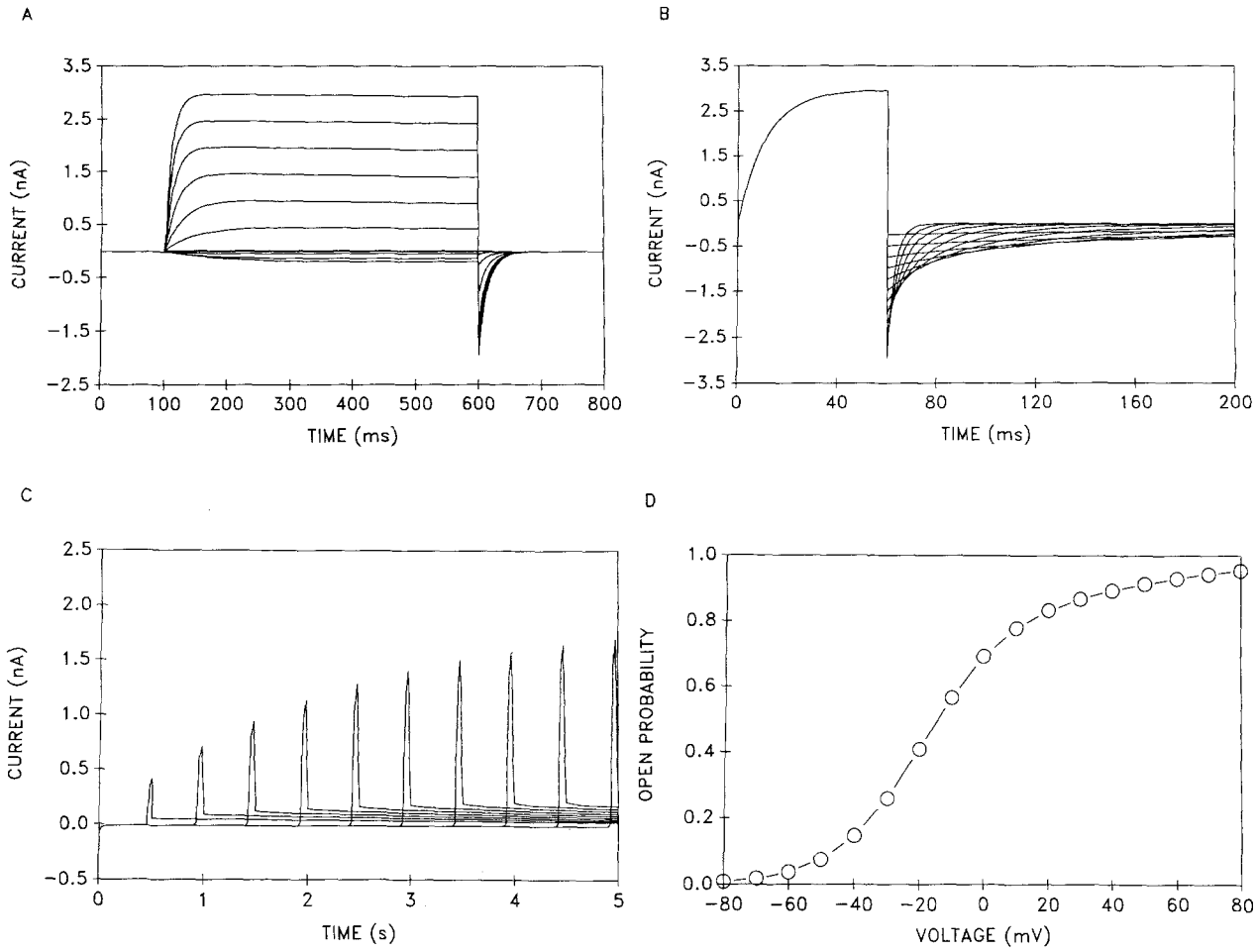

Fig. 11. (*A*) Model simulation of Fig. 2. (*B*) Model simulation of Fig. 8*A*. (*C*) Model simulation of Fig. 10*A*. (*D*) Model simulation of Fig. 5

cords. The single-channel conductance was approximately 150 pS in the negative voltage range. No currents could be recorded in the outward direction. The extrapolated reversal potential for this channel was greater than +50 mV. Considering the K^+ gradient that existed in this excised patch situation, the above is consistent with a K^+-selective channel. Given the similarities to the Ca^{2+}-activated K^+ channel from fresh monolayers, it is tentatively assumed that this was the same channel.

Nonselective Cation Channel. The last current we report from these cells is seen in both fresh monolayers and in dissociated cultured cells. Figure 14*A* shows typical single-channel records at various voltages from an inside-out patch. The bath contained normal physiological saline and the pipette contained physiological saline in which the Na^+ was replaced with K^+. Figure 14*B* shows the single-channel current-voltage relationship obtained from these records. The conductance was about 35 pS at negative voltages. Since the reversal potential was near 0 mV this must be a nonselective cation channel. In fresh monolayers, the NSC channel is Ca^{2+} activated. The fact that the NSC channel from dissociated cells is rarely seen in on-cell recordings but is seen in patches excised into solutions containing 2.5 mM Ca^{2+}, is consistent with a Ca^{2+} requirement for activation.

Discussion

The measured size of these cultured cells (31 μm), although large compared to measurements from freshly isolated lenses, is in agreement with reports from other cultured human lens epithelium. Brown and Bron (1987) reported a mean cell diameter of 12.7 μm for the human epithelium in intact lenses. Stewart et al. (1988) found a mean cell diameter of

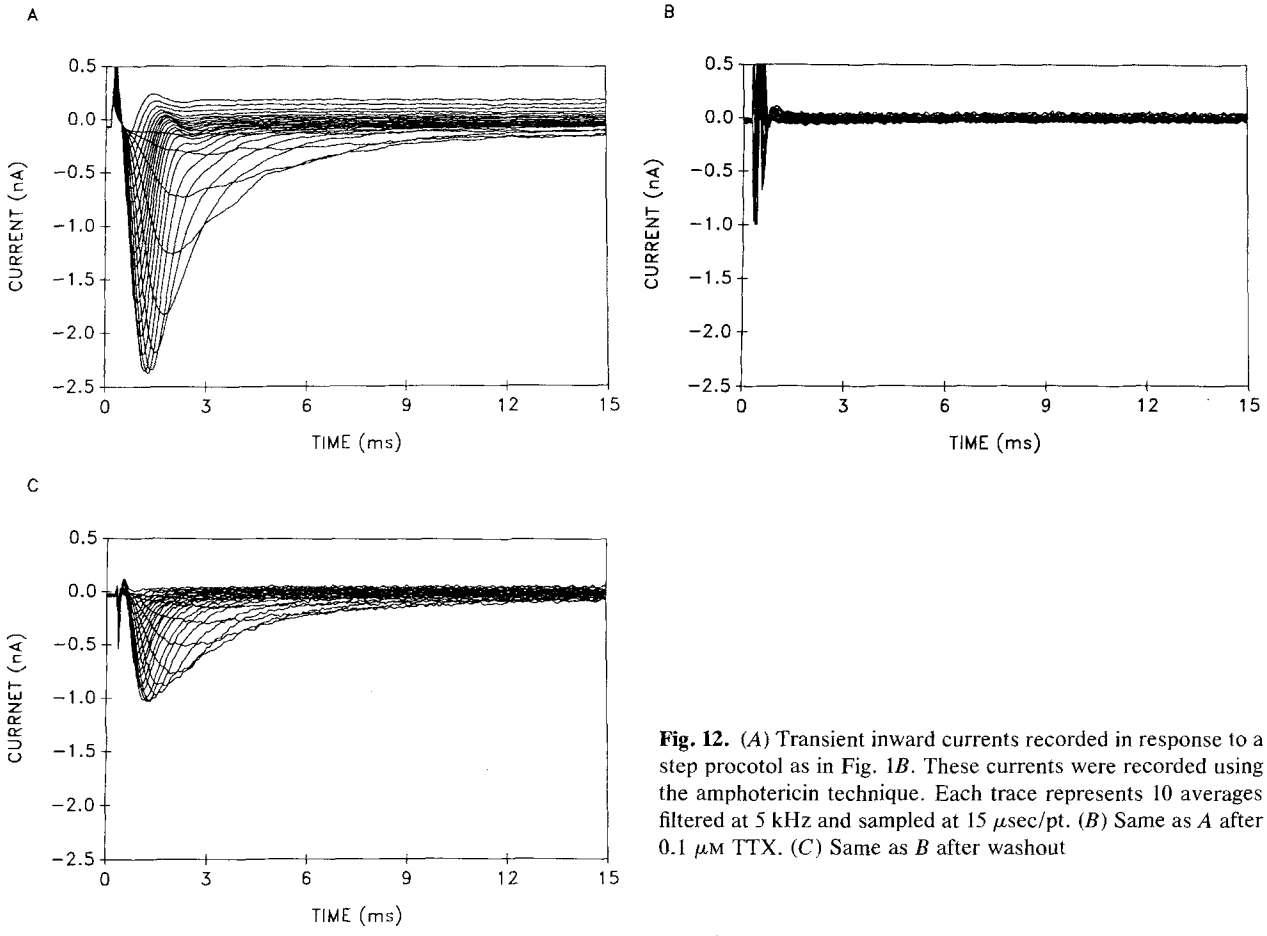

Fig. 12. (*A*) Transient inward currents recorded in response to a step procotol as in Fig. 1*B*. These currents were recorded using the amphotericin technique. Each trace represents 10 averages filtered at 5 kHz and sampled at 15 μsec/pt. (*B*) Same as *A* after 0.1 μM TTX. (*C*) Same as *B* after washout

about 30 μm in their cultured human lenses when grown to confluence. Our capacitance measurements agree roughly with these estimates of cell size but indicate that some cells had more capacitance than would have been expected from a simple measure of cell diameter.

The mean resting voltage of −19 mV recorded from these cells compares favorably with most other reports for human lens epithelium. Patmore and Maraini (1986) reported a resting voltage of −21 mV for whole human lenses. Jacob (1988) reported resting voltages between −20 and −24 mV for dissociated cultured human lens cells but values around −30 mV for fresh monolayers and nondissociated cultured cells. Stewart et al. (1988) reported resting voltages of −26 mV for their cultured human lens epithelial cells. It should be noted that the resting voltage measured using the whole-cell recording technique is heavily influenced by the composition of the pipette solution. Our pipette solutions were designed to reproduce the normal cytoplasmic ionic conditions as closely as possible given the uncertainty in present knowledge of that composition. Our cells had larger input resistances than most reported values. Stewart et al. (1988) report values of about 10 MΩ for individual cultured lens epithelial cells, while Jacob (1988) obtained values of about 150 MΩ. Both values are much lower than the 2.5-GΩ resistance we obtained. The low resistance measurements were made with traditional microelectrode techniques and may have underestimated the resistance due to the leakage commonly associated with microelectrode impalement. Consistent with this is the result stated by Jacob (1988) that whole-cell recordings from his isolated cells gave input resistances around 3 GΩ.

We identified four currents in these cells: an outwardly rectifying K^+ current, a large conductance (tentatively identified as Ca^{2+} activated) K^+ channel, a TTX-blockable Na^+ current, and a 35-pS NSC channel. The NSC and K^+ channels are similar to channels seen in fresh monolayers of human lens epithelium. We have not yet seen single channels corresponding to the two whole-cell currents reported here.

The most prominent whole-cell current seen in these cells was the outwardly rectifying K^+ current. The outward rectification was due to gating since, in

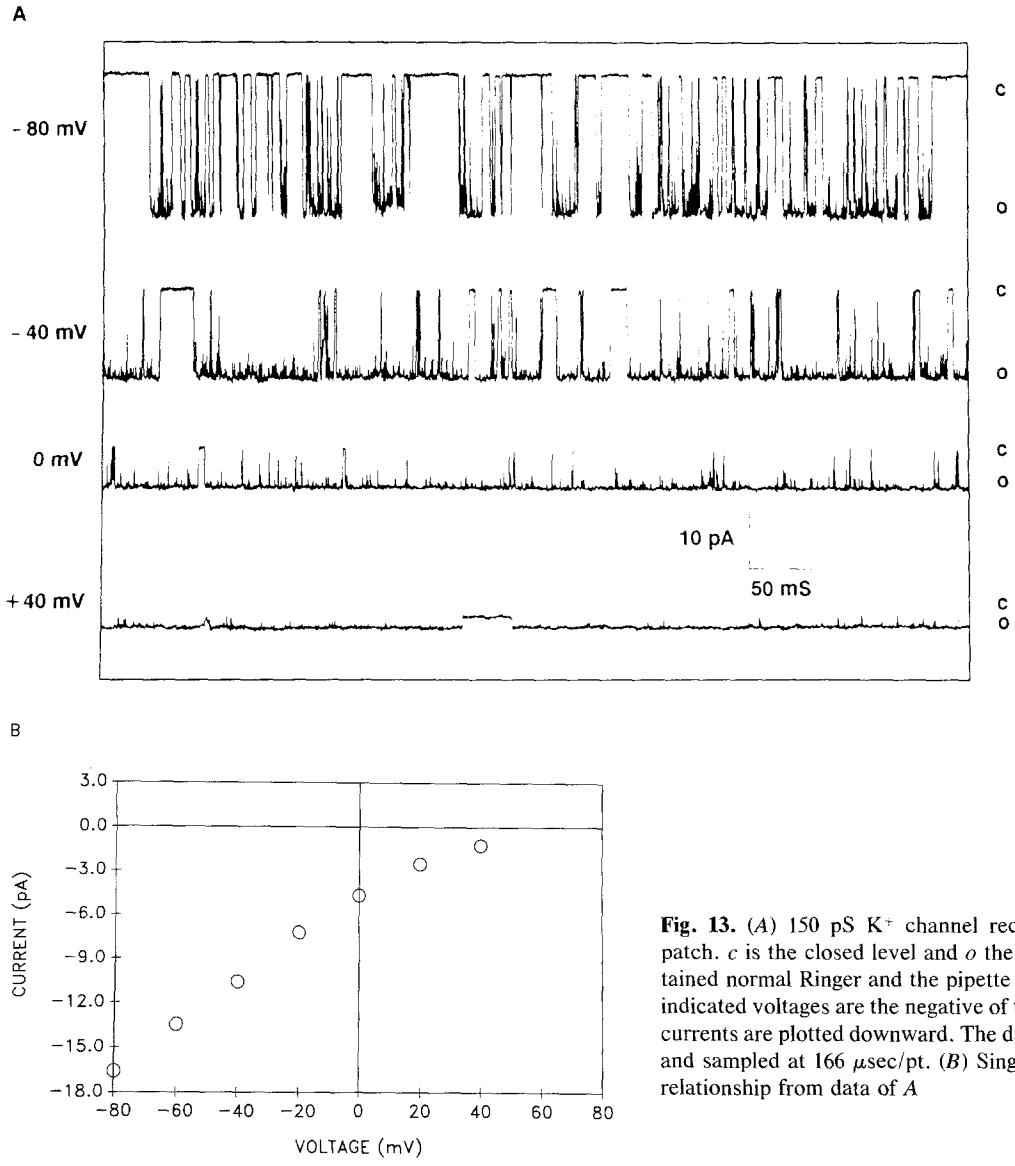

Fig. 13. (*A*) 150 pS K^+ channel recorded from an inside-out patch. *c* is the closed level and *o* the open level. The bath contained normal Ringer and the pipette contained K^+ Ringer. The indicated voltages are the negative of the pipette voltage. Inward currents are plotted downward. The data were filtered at 2.5 kHz and sampled at 166 μsec/pt. (*B*) Single-channel current-voltage relationship from data of *A*

symmetrical K^+ solutions, the instantaneous current-voltage relationship was linear. This current showed complex activation and inactivation kinetics. The basic kinetic behavior could be reproduced by a simple open-closed-inactivated model. However, a more complex model would be required to adequately reproduce the time-dependent behavior of the current in detail.

The simple three-state model predicts that the true steady-state open probability of this current (as opposed to the open probability of Fig. 5) is:

$$p = \frac{1}{1 + \frac{\gamma}{\delta} + \frac{\beta}{\alpha}}. \tag{5}$$

In the experiment shown in Fig. 5 the conditions are such that $\gamma/\delta = 0$. From the equations for the rate constants we can compute p as shown in Fig. 15. It is interesting that the peak of this curve is close to the measured resting voltage. Given the small amount of current measured in the vicinity of the resting voltage and the predicted value of p, it is plausible that the outwardly rectifying K^+ conductance has a role in setting the resting voltage of these cells. However, given that the resting voltage is only −20 mV there must be some other conductance holding these cells at a depolarized voltage. The identity of this conductance is unknown.

We have as yet no evidence of single-channel activity that would be consistent with the outwardly rectifying K^+ current. Even when the amount of

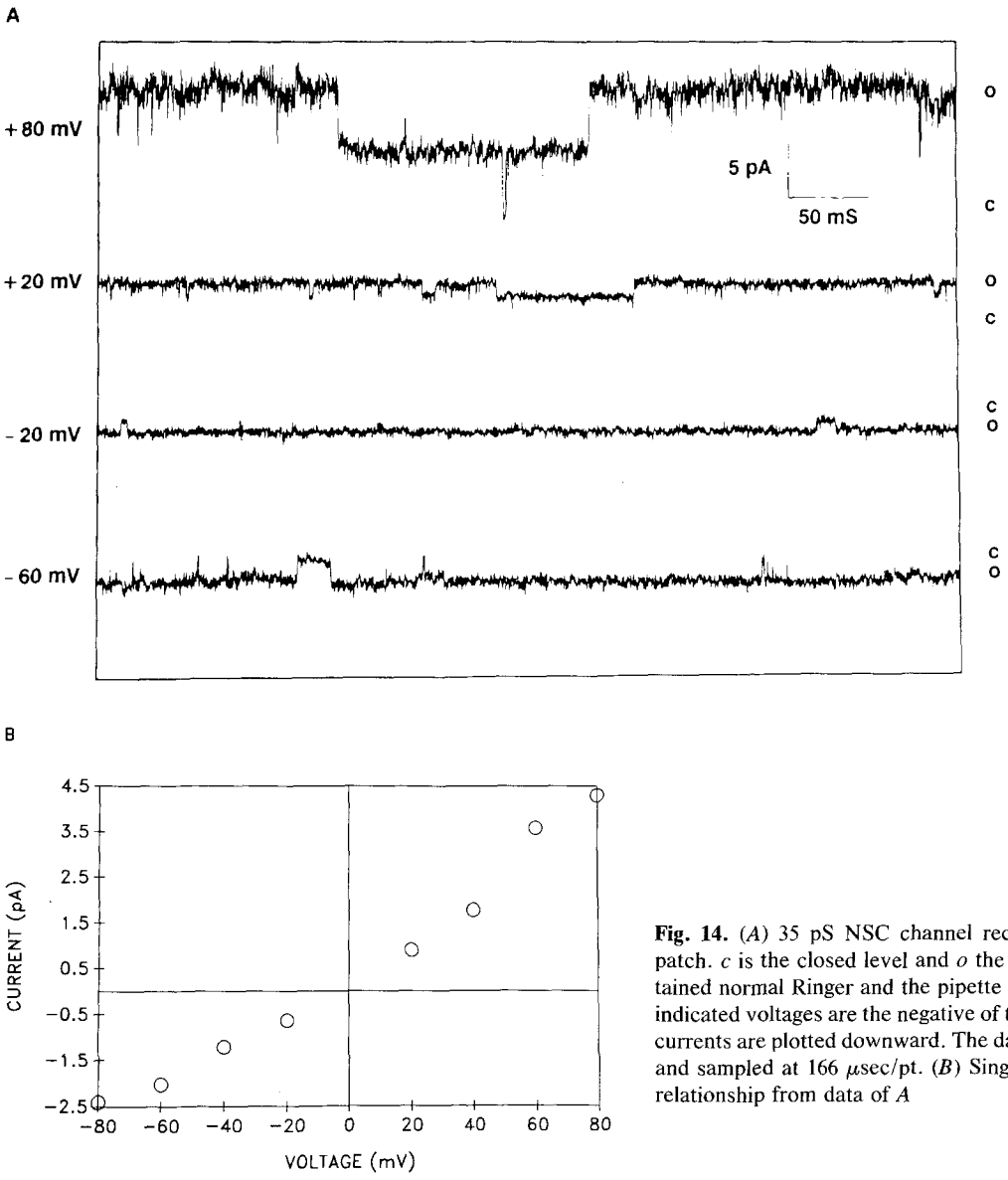

Fig. 14. (*A*) 35 pS NSC channel recorded from an inside-out patch. *c* is the closed level and *o* the open level. The bath contained normal Ringer and the pipette contained K^+ Ringer. The indicated voltages are the negative of the pipette voltage. Inward currents are plotted downward. The data were filtered at 2.5 kHz and sampled at 166 μsec/pt. (*B*) Single-channel current-voltage relationship from data of *A*

this current in a cell was small clear evidence of single-channel events in the whole-cell currents was not observed. If only a few channels were active, a large variance would be expected in the whole-cell currents. From this it seems possible that the single-channel conductance is small and that may explain why it was not seen in these cultured cells or in previous experiments with fresh monolayers. It is interesting that macroscopic measurements of membrane current from whole fresh monolayers show an outwardly rectifying macroscopic current-voltage relationship (Stewart et al. 1988).

The TTX-blockable Na^+ current is similar to that seen in excitable cells. In addition to the work reported here, we have also seen analogous Na^+ currents in another strain of cultured human lens epithelium and in cultured human nonpigmented ciliary body cells (both provided by Dr. Jon Polansky). Recently, Fain and Farahbakhsh (1989) have reported TTX-blockable Na^+ currents in cultured rabbit pigmented ciliary body cells. It is not clear what role such currents would have in the lens epithelium. The presence of Na^+ channels in these preparations might be due to dedifferentiation or some other artifact of cell culture (Freshney, 1987). This hypothesis can be tested if a viable preparation of primary human lens epithelial dissociates can be produced.

The K^+ channel seen in both fresh monolayers and in these cultured cells is likely a Ca^{2+}-activated K^+ channel. Such channels are ubiquitous in their occurrence but their function has only been eluci-

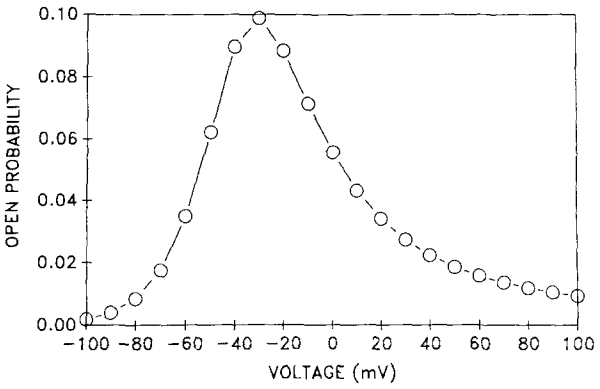

Fig. 15. Steady-state open probability as determined from the model of Eq. (3) and the experimentally determined voltage dependence of the rate constants

dated in a few systems (Blatz & Magleby, 1987). It appears they may play some role in cell volume regulation (Christensen, 1987; Hoffmann & Simonsen, 1989). The lack of a whole-cell current component corresponding to these channels is not unexpected. The open probability of such channels is essentially negligible at the voltages and internal Ca^{2+} concentrations used in these experiments.

The 35-pS NSC channel seen in both fresh monolayers and in cultured cells may also be Ca^{2+} activated. The presence of NSC channels in a wide variety of cell types has been demonstrated (Partridge & Swandulla, 1988). As with the Ca^{2+}-activated K^+ channel, the role of the NSC channel in the normal physiology of the cell is not well understood. Such channels have been seen in every lens epithelial preparation so far investigated (Rae et al., 1988).

Only one other report of channels in human lens epithelium has appeared (Jacob, 1988). The channels reported by Jacob do not appear to be the same as seen in our preparation. Using on-cell patches with physiological saline in the pipette, Jacob reported a 49-pS K^+ channel, a 14-pS Cl^- channel, and a 25-pS nonselective cation channel. Differences in cell culture procedures may account for the different channel types seen in Jacob's study *versus* our study.

There are certain potential problems associated with the cell culture and whole-cell clamp techniques that need to be addressed. In any study of cultured cells, the issues of loss of cellular differentiation and contamination by other cell types must be considered. The lens epithelium is a favorable preparation from the standpoint of contamination. By culturing only the central lens epithelium, one is dealing with a population containing only a single cell type. The question of loss of differentiated function is a more difficult problem. It would be valuable to have some tissue-specific function to assay as a test for dedifferentiation. One highly specific function that could be tested for in lens epithelial cells is the presence of the lens-specific protein α-crystallin. We have not yet done such tests with our cultured cells.

The fact that these cells were studied in a dissociated state means that they may have lost any inherent polarity that was present in the monolayer. However, unless there is some mechanism that causes the cells to rapidly remove transporters from the membrane when polarity is lost, whole-cell currents should still be produced by any channels present in the cell. Since we are not making statements about the location (apical *vs.* basolateral) of these channels, loss of polarity is not a concern. Ultimately, the combination of single-channel work on intact monolayers and whole-cell recording on dissociated cells should allow localization of conductances to apical *vs.* basolateral membranes.

Finally, the problem of washout in whole-cell recording has been controlled for here by the use of the perforated-patch technique. No differences were seen between the perforated-patch recordings and traditional whole-cell recordings, and thus there is no evidence of loss of important control molecules from these cells during recording.

The major result of this paper is that these cultured human lens epithelial cells contain an outwardly rectifying K^+ conductance that has the necessary properties to play an important role in setting resting voltage. This is, to the best of our knowledge, the first direct identification of a current responsible for the resting voltage of any lens epithelium. Certainly further experimentation will be necessary to establish the connection between the outwardly rectifying K^+ conductance and resting voltage.

We would like to acknowledge the assistance of Helen Hendrickson who established and maintained the cell cultures used in these studies. Also we would like to thank Erika Wohlfiel for her expert secretarial services and Dr. Mitchell Watsky for many useful discussions and comments on the manuscript. We thank Dr. Jon Polansky for providing samples of his cultured human lens and ciliary body cells. Finally, we thank the Mayo Foundation Eye Bank for providing us with human lenses for these studies. This work was supported by NIH grants EY03282, EY06005 and an unrestricted award from Research to Prevent Blindness.

References

Bezanilla, F. 1985. A high capacity data recording device based on a digital audio processor and a video cassette recorder. *Biophys. J.* **47**:437–441

Blatz, A.L., Magleby, K.L. 1987. Calcium-activated potassium channels. *Trends Neurosci.* **10:**463–467

Brown, N.A.P., Bron, A.J. 1987. An estimate of the human lens epithelial cell size in vivo. *Exp. Eye Res.* **44:**899–906

Christensen, O. 1987. Mediation of cell volume regulation by Ca^{2+} influx through stretch-activated channels. *Nature (London)* **330:**66–68

Cooper, K., Rae, J.L., Gates, P. 1989. Membrane and junctional properties of dissociated frog lens epithelial cells. *J. Membrane Biol.* **111:**215–227

DeCoursey, T.E., Jacobs, E.R., Silver, M.R. 1988. Potassium currents in rat type II alveolar epithelial cells. *J. Physiol. (London)* **395:**487–505

Ermishkin, L.N., Kasumov, Kh.M., Potzeluyev, V.M. 1976. Single ionic channels induced in lipid bilayers by polyene antibiotics amphotericin B and nystatine. *Nature (London)* **262:**698–699

Fain, G.L., Farahbakhsh, N.A. 1989. Voltage-activated currents recorded from rabbit pigmented ciliary body epithelial cells. *J. Physiol. (London)* **417:**83–103

Freshney, R.I. 1987. Culture of Animal Cells: A Manual of Basic Technique. Alan R. Liss, New York

Gogelein, H. 1988. Chloride channels in epithelia. *Biochim. Biophys. Acta* **947:**521–547

Hamada, Y., Okada, T.S. 1978. In vitro differentiation of cells of the lens epithelium of human fetus. *Exp. Eye Res.* **26:**91–97

Hoffmann, E.K., Simonsen, L.O. 1989. Membrane mechanisms in volume and pH regulation in vertebrate cells. *Physiol. Rev.* **69:**315–382

Horn, R., Marty, A. 1988. Muscarinic activation of ionic currents measured by a new whole-cell recording method. *J. Gen. Physiol.* **92:**145–159

Hunter, M., Oberleithner, H., Henderson, R.M., Giebisch, G. 1988. Whole-cell potassium currents in single early distal tubule cells. *Am. J. Physiol.* **255:**F699–F703

Jacob, T.J.C. 1988. Fresh and cultured human lens epithelial cells: An electrophysiological study of cell coupling and membrane properties. *Exp. Eye Res.* **47:**489–506

Lindau, M., Fernandez, J.M. 1986. IgE-mediated degranulation of mast cells does not require opening of ion channels. *Nature (London)* **319:**150–153

Marty, A., Neher, E. 1983. Tight-seal whole-cell recording. *In:* Single-Channel Recording. B. Sakmann and E. Neher, editors. pp. 107–122. Plenum, New York

McCann, J.D., Welsh, M.J. 1990. Regulation of Cl^- and K^+ channels in airway epithelium. *Annu. Rev. Physiol.* **52:**115–135

Nagineni, C.N., Bhat, S.P. 1989. Human fetal lens epithelial cells in culture: An in vitro model for the study of crystallin expression and lens differentiation. *Curr. Eye Res.* **8:**285–291

Palmer, L.G., Frindt, G. 1986. Epithelial sodium channels: Characterization by using the patch-clamp technique. *Fed. Proc.* **45:**2708–2712

Partridge, L.D., Swandulla, D. 1988. Calcium-activated non-specific cation channels. *Trends Neurosci.* **11:**69–72

Patmore, L., Maraini, G. 1986. A comparison of membrane potentials, sodium and calcium levels in normal and cataractous human lenses. *Exp. Eye Res.* **43:**1127–1130

Petersen, O.H. 1987. Electrophysiology of exocrine gland cells. *In:* Physiology of the Gastrointestinal Tract. L.R. Johnson, editor, pp. 745–771. Raven, New York

Petersen, O.H. 1989. Patch-clamp experiments in epithelia: Activation by hormones or neurotransmitters. *Methods Enzymol.* **171:**663–678

Press, B.P., Flannery, W.H., Teukolsky, S.A., Vetterling, W.T. 1986. Numerical Recipes: The Art of Scientific Computing. Cambridge University Press, Cambridge

Rae, J.L. 1984. The patch voltage clamp: Its application to lens research. *Lens Res.* **2:**61–87

Rae, J.L., Cooper, K. 1990. New techniques for the study of lens electrophysiology. *Exp. Eye Res. (in press)*

Rae, J.L., Dewey, J., Cooper, K. 1989. Properties of single potassium-selective ionic channels from the apical membrane of rabbit corneal endothelium. *Exp. Eye Res.* **49:**591–609

Rae, J.L., Levis, R.A. 1984. Patch voltage clamp of lens epithelial cells: Theory and practice. *Molec. Physiol.* **6:**115–162

Rae, J.L., Levis, R.A., Eisenberg, R.S. 1988. Ionic channels in ocular epithelia. *In:* Ion Channels. T. Narahashi, editor. pp. 283–327. Plenum, New York

Rae, J.L., Mathias, R.T. 1985. The physiology of the lens. *In:* The Ocular Lens: Structure, Function, and Pathology. H. Maisel, editor. pp. 93–121. Marcel Dekker, New York—Basel

Reddan, J.R., McGee, S.J., Goldenberg, E.M., Dziedzic, D.C. 1982/1983. Both human and newborn rabbit lens epithelial cells exhibit similar limited growth properties in tissue culture. *Curr. Eye Res.* **2:**399–405

Reddy, V.N., Lin, L.R., Arita, T., Zigler, J.S., Huang, Q.L. 1988. Crystallins and their synthesis in human lens epithelial cells in tissue culture. *Exp. Eye Res.* **47:**465–478

Stewart, S., Duncan, G., Marcantonio, J.M., Prescott, A.R. 1988. Membrane and communication properties of tissue cultured human lens epithelial cells. *Invest. Ophthalmol. Vis. Sci.* **29:**1713–1725

Welsh, M.L. 1987. Electrolyte transport by airway epithelia. *Physiol. Rev.* **67:**1143–1184

Wills, N.K., Zweifach, A. 1987. Recent advances in the characterization of epithelial ionic channels. *Biochim. Biophys. Acta* **906:**1–31

Received 2 February 1990; revised 3 April 1990